

# Antiproliferative activities of a library of hybrids between indanones and HDAC inhibitor SAHA and MS-275 analogues

Cédric Charrier,<sup>a</sup> Joëlle Roche,<sup>b</sup> Jean-Pierre Gesson<sup>a</sup> and Philippe Bertrand<sup>a,\*</sup>

<sup>a</sup>*Synthèse et Réactivité des Substances Naturelles, CNRS UMR 6514, Université de Poitiers, 40 Avenue du Recteur Pineau, Poitiers F-86022, France*

<sup>b</sup>*Institut de Physiologie et Biologie Cellulaires, CNRS UMR 6187, Université de Poitiers, 40 Avenue du Recteur Pineau, Poitiers F-86022, France*

Received 4 July 2007; revised 7 September 2007; accepted 8 September 2007  
Available online 14 September 2007

**Abstract**—New compounds derived from inhibitors of histone deacetylases (HDACs) have been synthesized and their antiproliferative activities towards non small lung cancer cell line H661 evaluated. Their design is based on hybrids between indanones to limit conformational mobility and other known HDAC inhibitors (SAHA, MS-275). The synthesis of these new derivatives was achieved by alkylation of appropriate indanones to introduce the side chain bearing a terminal ester group, the latter being a precursor of hydroxamic acid and aminobenzamide derivatives. These new analogues were found to be moderately active to inhibit H661 cell proliferation.

© 2007 Elsevier Ltd. All rights reserved.

In eukaryotic cells, the reversible packing of DNA in the chromatin structure provides the control of gene activation and repression. The fundamental element of the chromatin structure is the nucleosome, assembled from the highly conserved histone proteins H2A, H2B, H3, and H4, forming an octameric core around which the DNA is folded and sealed by histone H1.<sup>1</sup> The regions of chromatin that are involved in gene transcription, DNA replication, and DNA repair are actively remodeled by regulation of histone acetylation, methylation, phosphorylation, and ubiquitylation.<sup>2,3</sup> Acetylation and deacetylation of  $\varepsilon$ -amino group of specific histone lysines play a crucial role in the transcriptional process and deregulation can lead to cancer.<sup>4–6</sup> HATs (histone acetyl transferases) are responsible for the acetylation of lysines, while HDACs (histone deacetylases) activity lead to deacetylation.<sup>7</sup> Inhibition of HDACs elicits anticancer effects in several tumors by inhibition of cell growth and inducing cell differentiation.<sup>8</sup> It is now well established that a variety of proteins are also substrates for HDACs and at least 50 non histone proteins of known biological functions have been identified,<sup>9,10</sup> with functions beyond the alteration of chromatin struc-

tures.<sup>11</sup> Therefore, inhibiting HDAC is an attractive target for anticancer therapy.<sup>12–14</sup> Several programs for the development of HDAC inhibitors (HDI) as anticancer drugs have been initiated.<sup>11,15</sup> Trichostatin A **1**<sup>16</sup> (Fig. 1), a natural product isolated from *Streptomyces hygroscopicus*, was later reported as HDI.<sup>17</sup> Synthetic analogues, like SAHA **2**,<sup>18</sup> MS-275 **3**, and NVP-LAQ824 **4**, are in clinical trials.<sup>19</sup> SAHA was recently approved for treatment of cutaneous T-cell lymphoma.<sup>20</sup> HDI activities requires (1) a functional group

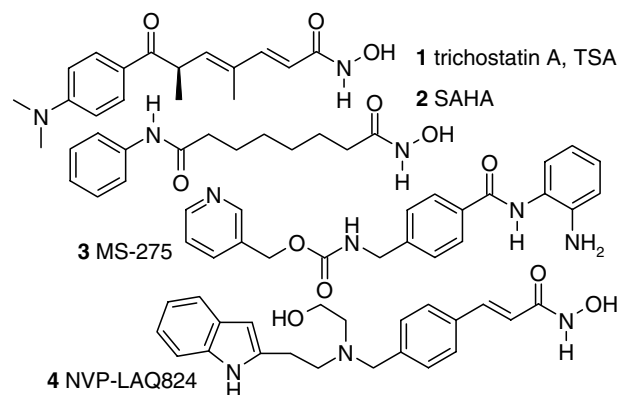


Figure 1. Natural and synthetic HDI.

**Keywords:** Histone deacetylase; Cancer; Epigenetic; Trichostatin A; SAHA; MS-275; Indanones; Hybrid.

\* Corresponding author. E-mail: [philippe.bertrand@univ-poitiers.fr](mailto:philippe.bertrand@univ-poitiers.fr)

able to chelate the metal atom at the bottom of the active site, (2) a recognition moiety interacting with the external surface of the protein, and (3) a spacer linking these two moieties and fitting the tubular geometry of this site.

Crystallographic data are available describing the binding mode to HDLP or HDAC8 for TSA **1**, SAHA **2**,<sup>21</sup> MS-344 **5**,<sup>22</sup> and the benzohydroxamate **6**<sup>23</sup> (Fig. 2). In each case, the aromatic ring of **1**, **3**, **5** and the pyridyl moiety of **6** are located at the external surface of the active site. Effective HDI with large recognition elements such as **9** were also described.<sup>22</sup> For TSA, SAHA, and MS-344, the intermediate chain is stacked between two phenylalanines (Phe141 and Phe198 in HDLP), the hydroxamic acid function chelating the zinc. In compound **6**, the thiophenesulfonamide part behaves as the aryl chain of SAHA.

We previously described the synthesis of the racemic rigid TSA analogue **7**.<sup>24</sup> This compound possesses antiproliferative activities ( $IC_{50} = 0.3 \mu M$ ) on H661 cells and HDI activity. The dimethylamino group present on the aromatic ring was essential to achieve these high activities, as the unsubstituted homologue was found 10-fold less active.

In the present work, we prepared hybrid compounds between known HDI like SAHA or MS-275 and the indanone moiety of compound **7** by replacement of the butadien chain with aliphatic or aryl spacers. Hydroxamic acid and benzamide groups were selected as  $Zn^{2+}$  chelating functions for each new derivative.

For aliphatic analogues we selected a chain length in the range of four to six carbons, as in TSA and SAHA, respectively (Fig. 3,  $X = (CH_2)_{3-5}$ ). Aromatic spacers were designed to keep the original arrangement of the methylbutadienyl group and the insaturations of TSA or **7**. Thus a ring closure was envisioned between the methyl group of the dien chain and the carbon adjacent to the carbonyl group of the hydroxamic acid. This led to 1,3 disubstituted aromatic rings. A benzyl group was first selected (Fig. 3,  $X = Ph$ ). Compounds like **10** being described as HDI,<sup>25</sup> a methylthiazolyl group (Fig. 3,  $X = thiazol$ ) was also retained. Although our aromatic spacers are 1,3 disubstituted, they are similar to spacers of **6** and **9**. Interestingly, unsubstituted *para*-benzamide **8** (Fig. 2) without a methyl at  $C_2$  was described with antiproliferative activity on HCT116 cells

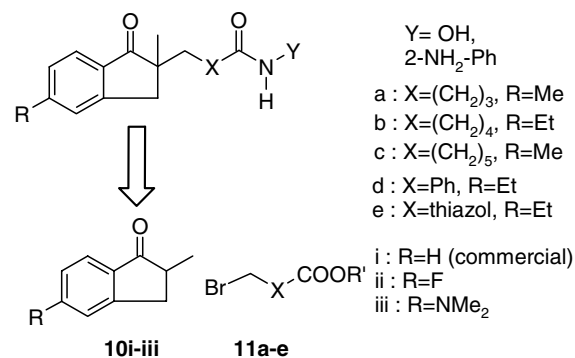
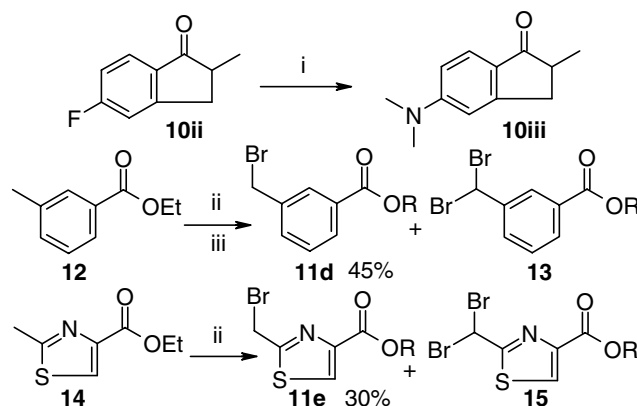


Figure 3. Aliphatic and aromatic indanones analogues.

( $IC_{50} = 0.9 \mu M$ ).<sup>26</sup> Preparation of this library involves the alkylation of indanones by convenient halogenated esters. Hydroxamic acid and benzamide groups can then be accessed from these esters. This strategy allows separate preparation of the required indanones **10i-iii** and halogenated esters **11a-e** (Fig. 3).

Indanone **10ii** was prepared according to known procedure.<sup>27</sup> Nucleophilic aromatic substitution of **10ii** afforded **10iii** (Scheme 1) in 75% yield.<sup>28</sup> Previous work showed that a fluorine atom at the indanone aromatic ring does not lead to an increase of activity. Thus the intermediate **10ii** (Fig. 3, R = F) was not used to prepare fluorinated analogues. Bromoalkyl chains were commercially available as ethyl bromoesters **11a, b**, and **c** was prepared by known procedure.<sup>29</sup> The halogenated aro-



Scheme 1. Reagents: (i) DMSO:H<sub>2</sub>O, K<sub>2</sub>CO<sub>3</sub>, Me<sub>2</sub>NH·HCl, 75%; (ii) NBS, CCl<sub>4</sub>, BzO<sub>2</sub>; (iii) NEt<sub>3</sub>, (EtO)<sub>2</sub>PHO.

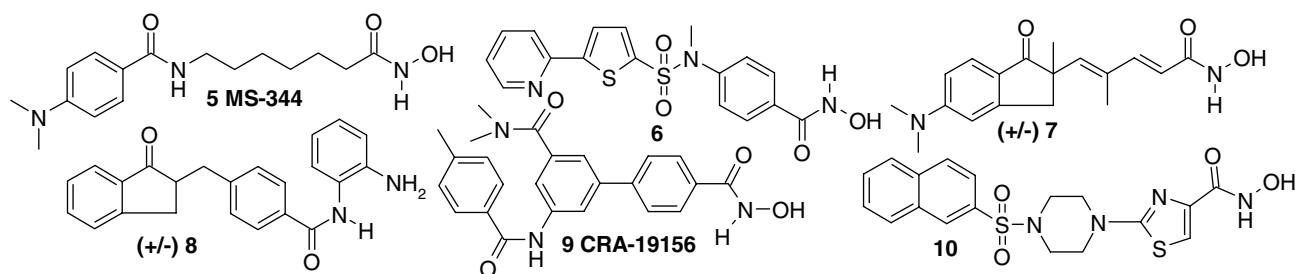
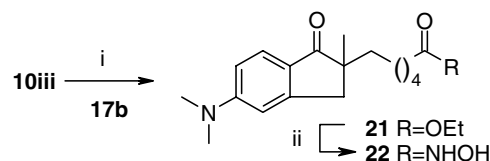


Figure 2. Examples of alkyl, aryl, and thiazolyl HDI.

matic counterparts were prepared by bromination. Benzoate **12** afforded inseparable mono- and dibromo derivatives **11d** and **13**. Mono debromination of the mixture finally gave **11d** in 45% yield.<sup>30</sup> The same strategy applied to **14** gave the two separable mono- and dibrominated compounds **11e** and **15**. Alkylation of **10i** with bromides **11d,e** afforded aromatic esters **16d,e**, while bromides **11a–c** were found unreactive (Scheme 2), even when HMPA was used.

Conversion of **11a–c** to the corresponding iodides **17a**,<sup>31</sup> **17b**,<sup>32</sup> and **17c**<sup>29</sup> (Scheme 2), followed by alkylation, finally gave the expected esters **16a–c** in good yields. Esters **16a–e** were converted to acids **18a–e** (Scheme 3) and upon coupling with NH<sub>2</sub>-OTHP and subsequent hydrolysis afforded hydroxamic acids **19a–e**. Aminobenzenamides **20a–e** were obtained by coupling **18a–e** with 1,2-diaminobenzene.

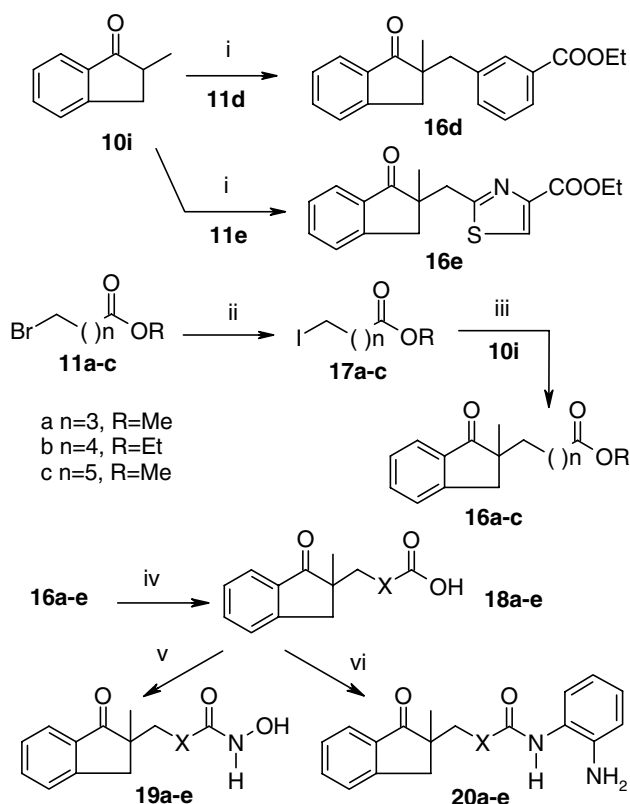
In order to compare the activity of unsubstituted and substituted indanone, attempts were made to alkylate **10iii** with ester **17**. As LDA alkylation protocol failed, other bases were evaluated for the deprotonation (NaH, THF, or NaH, dimethoxyethane), NaHMDS in THF giving the best results despite the rather modest yield (40%), but unreacted **10iii** can be partially recovered. Treatment of ester **21** in a mixture of DMF or EtOH, and 50% aqueous NH<sub>2</sub>OH for 5 days gave



**Scheme 3.** Reagents and conditions: (i) NaHMDS, THF,  $-70^{\circ}\text{C}$ , 38%; (ii) EtOH, NH<sub>2</sub>OH 50% aq, 5 days, 45%.

hydroxamic acid **22** with a yield of 45%. Due to experimental difficulties from this latter short strategy and the modest overall yields, other alkylated derivatives of **10iii** were not prepared.

New derivatives were tested for tumor cell antiproliferative activity as this effect is well known for HDI and is an important parameter for further development. After 48 h treatment of non small cell lung cancer H661 cells, IC<sub>50</sub> values (Table 1) were determined and compared to TSA or SAHA (Figure 6, Supplementary data). In the aromatic series, compounds **19d,e** and **20d,e** do not show any activity at 25  $\mu\text{M}$  (the highest tested concentration). Some alkylated analogues showed a modest activity, with compounds **19c** and **20b** having IC<sub>50</sub> value of 20  $\mu\text{M}$ . Compounds **19a**, **20a**, and **20c** are active but



**Scheme 2.** Reagents and conditions: (i) LDA, THF,  $-78^{\circ}\text{C}$ , 68–93%; (ii) NaI, acetone, 98%; (iii) LDA, THF,  $-78^{\circ}\text{C}$ , HMPA, 88–95%; (iv) LiOH, MeOH; 95% (v) a—H<sub>2</sub>N-OTHP, TBTU, DMF, NEt<sub>3</sub>; b—CSA, CH<sub>2</sub>Cl<sub>2</sub>, MeOH, 36–60% (a + b); (vi) H<sub>2</sub>N-Ph-NH<sub>2</sub>, EDC, THF, 73–85%.

**Table 1.** Antiproliferative activities of **1**, **2** and new TSA and SAHA analogues **19a–e**, **20a–e** and **22** against H661 cells after 48 h treatment

Compound	IC <sub>50</sub> $\mu\text{M}$			
<b>1</b> (TSA)	0.085			
<b>2</b> (SAHA)	5			
	R	X	Y	
<b>19a</b> (IC4H)	H	(CH <sub>2</sub> ) <sub>3</sub>	OH	>25
<b>19b</b> (IC5H)	H	(CH <sub>2</sub> ) <sub>4</sub>	OH	NA
<b>19c</b> (IC6H)	H	(CH <sub>2</sub> ) <sub>5</sub>	OH	20
<b>19d</b> (IBH)	H		OH	NA
<b>19e</b> (ITH)	H		OH	NA
<b>20a</b> (IC4B)	H	(CH <sub>2</sub> ) <sub>3</sub>	Ph-NH <sub>2</sub>	>25
<b>20b</b> (IC5B)	H	(CH <sub>2</sub> ) <sub>4</sub>	Ph-NH <sub>2</sub>	20
<b>20c</b> (IC6B)	H	(CH <sub>2</sub> ) <sub>5</sub>	Ph-NH <sub>2</sub>	≥25
<b>20d</b> (IBB)	H		Ph-NH <sub>2</sub>	NA
<b>20e</b> (ITB)	H		Ph-NH <sub>2</sub>	NA
<b>22</b> (Me <sub>2</sub> N-IC5H)	Me <sub>2</sub> N	(CH <sub>2</sub> ) <sub>4</sub>	OH	NA

IC<sub>50</sub> were determined from the curves of antiproliferative activities (Figure 6, Supplementary data) at the concentration required for 50% inhibition of cell proliferation. Experiments were done in triplicate. NA, no activity detected at the maximum tested concentration (25  $\mu\text{M}$ ).

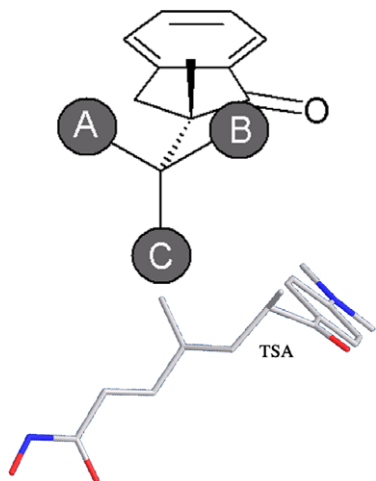


**Figure 4.** Possible orientations of spacers linked to the indanone moiety and TSA bound to HDAC8 in conformation A.

IC<sub>50</sub> values could not be determined because at the highest concentration (25  $\mu$ M), inhibition was less than 50%. The expected improvement of activity for compound **22**, compared to its unsubstituted homologue **19b**, was not obtained. Observed activities were then analyzed in relation with the structure of SAHA and compounds **6** and **9** bound to HDAC8. Thus compounds **19b–e** were iteratively submitted to molecular dynamics (MM2 method) and then optimized (AM1 level) until stable conformers were obtained.

Three orientations A, B, and C of the spacer relative to the indanone were considered (Fig. 4), A being adopted by the chain of TSA and **7**. 3D structures of *para*-benzohydroxamates being only accessible, the *para* equivalent of **19d** was modeled for comparative purposes. Several stable conformers were obtained in each case. Conformers of **19d** and for the *para* derivatives of **19d** gave analogous conformations, the position of the hydroxamic acid function on the phenyl ring having little impact on the stability. All conformers were first

compared to the structure of HDI obtained from crystallographic data (Figure 7, Supplementary data) and then docked in the active site of HDAC8.<sup>33</sup> The key parameters for comparison studies were the overlapping of the hydroxamic acids, the fitting of the aliphatic chains and carbonyl group of indanone for **19b,c** with SAHA, and the overlapping of the aromatic ring for **19d** and **19e** with **6** or **9**.

Conformers of **19b** compared to SAHA (Figure 8, Supplementary data) gave interactions with the surface while conformer c6c of **19c** did not (Fig. 5A). The chain of SAHA presents a particular folding shortening the distance between the carbonyl of the amide group and the hydroxamic acid. Conformers c5a and c6c were remodeled according to this folding, although not giving the most stable conformers (Fig. 5B and C). Similarly to the optimized conformers, the C<sub>2</sub> methyl group in **19b** gave interaction with the surface while **19c** did not. **19a** is probably too short to fold as SAHA, with a methyl group close to the entry of the site and is not planar enough to compete with TSA or **7**. These results appeared consistent with the observed activities for **19c** compared to **19a,b**. The activity of hybrid **19c** is probably due to the flexible nature of the aliphatic chain. Despite the sterics of the methyl group at C<sub>2</sub>, the length of this chain appears to be optimal. Compound **20b** is active (25  $\mu$ M), while hydroxamate **19b** is not, suggesting that in this case the benzamide group compensates the shorter chain length.

In the case of **19d** compared to **6** or **9** conformation A is obtained for conformers mb2 and mb3, with different orientations of the hydroxamic acid (Figures 9 and 10, Supplementary data). Results for the *para* derivative of **19d** are almost identical. Conformer mb3 of **19d** gave conformational similarity to TSA (Fig. 5D) validating our initial hypothesis for the design of 1,3 disubstituted spacers. Despite this, the orientation of the phenyl ring, compared to the butadien system of TSA or **7**, gave interactions in the tubular access. In addition, the inter-

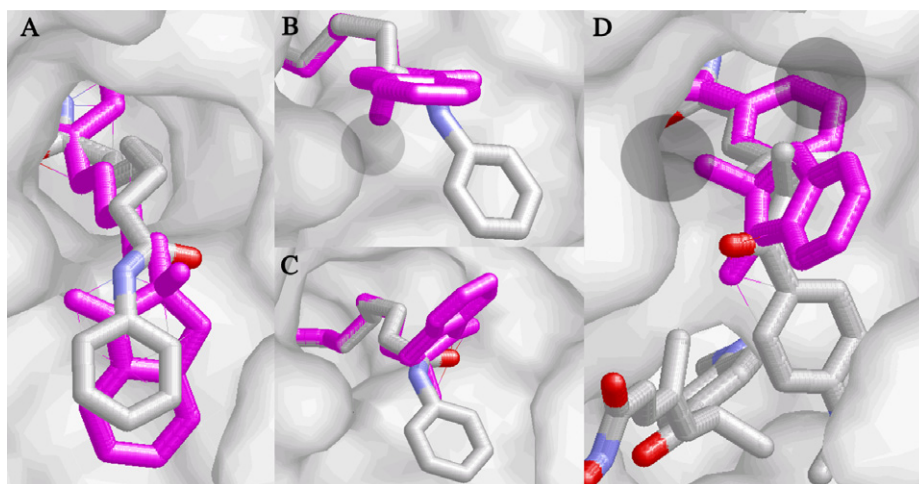


**Figure 5.** Comparison of the binding modes in the active site of HDAC8. (A) SAHA (CPK) and conformer c6c of **19c** (pink); (B and C) remodeled conformers c5a (B) and c6c (C) according to the folding of SAHA; (D) TSA (CPK) and conformer mb3 of **19d** (pink). Grey areas show interactions with the surface of the site.



action resulting from the methyl group can explain the lack of activity compared to TSA or to the aliphatic compound **19c**. Conformers of **19e** are preferentially in the A or C conformations probably to avoid recovering of doublets between the oxygen atom of indanone and the sulfur atom of the thiazol. The smaller ring size, compared to phenyl, increased interactions, except for t1 (Figure 11, Supplementary data).

In conclusion, hybrid molecules designed between indanones and MS-275 or SAHA derivatives were prepared. Only hybrid analogues of SAHA showed antiproliferative activities. In contrast to *para*-benzohydroxamate like MS-275 or **6**, our derivatives based on *meta*-benzohydroxamate and thiazolyl derivatives do not show substantial activity. In this study, we measured antiproliferative activity as a screening test of our new compounds. With this approach, we could determine the parameters for the interactions of our indanones' derivatives with the protein surface of HDAC8. When large spacers were used to link the chelating function to the indanone, major interactions were obtained. For 1,3 disubstituted aromatic spacers, the link between this spacer and the indanone system should be longer than a methylene group, with at least two atoms, such as the sulfonamide link of compound **6**. Local minor interactions were observed with the methyl group at position C<sub>2</sub> in both the aliphatic and aromatic groups of analogues. Thus this methyl group should be removed to allow easier access to the active site. Therefore, compound **19c** is a promising candidate for further modifications and for estimation of HDAC inhibitory activities.

### Acknowledgments

We thank MENRT, CNRS, and La Ligue Contre le Cancer, Comité de Charente-Maritime for financial support.

### Supplementary data

Supplementary data associated with this article can be found, in the online version, at [doi:10.1016/j.bmcl.2007.09.041](https://doi.org/10.1016/j.bmcl.2007.09.041).

### References and notes

- Chakraborty, S.; Senyuk, V.; Nucifora, G. *J. Cell. Biochem.* **2001**, *82*, 310.
- Kouzarides, T. *Cell* **2007**, *128*, 693.
- Li, B.; Carey, M.; Workman, J. L. *Cell* **2007**, *128*, 707.
- Cairns, B. R. *Trends Cell Biol.* **2001**, *11*, 15.
- Lund, A. H.; van Lohuizen, M. *Genes Dev.* **2004**, *18*, 2315.
- Jones, P. A.; Baylin, S. B. *Cell* **2007**, *128*, 683.
- Yang, X.-J.; Seto, E. *Curr. Opin. Genet. Dev.* **2003**, *13*, 143.
- Marks, P. A.; Rifkind, R. A.; Richon, V. M.; Breslow, R.; Miller, T.; Kelly, W. K. *Nat. Rev. Cancer* **2001**, *1*, 194.
- Xu, W. S.; Parmigiani, R. B.; Marks, P. A. *Oncogene* **2007**, *26*, 5541.
- Xang, X. J.; Seto, E. *Oncogene* **2007**, *26*, 5310.
- (a) Minucci, S.; Pelicci, P. G. *Nat. Rev. Cancer* **2006**, *6*, 38; (b) Lin, H.-Y.; Chen, C.-S.; Lin, S.-P.; Weng, J.-R.; Chen, C.-S. *Med. Res. Rev.* **2006**, *26*, 397.
- Johnstone, R. W. *Nat. Rev. Drug Disc.* **2002**, *1*, 287.
- Somech, R.; Izraeli, S.; Simon, A. J. *Cancer Treat. Rev.* **2004**, *30*, 461.
- Mai, A.; Massa, S.; Rotili, D.; Cerbara, I.; Valente, S.; Pezzi, R.; Simeoni, S.; Ragno, R. *Med. Res. Rev.* **2005**, *25*, 261.
- Monneret, C. *Eur. J. Med. Chem.* **2005**, *40*, 1.
- Tsuji, N.; Kobayashi, M.; Nagashima, K.; Wakisaka, Y.; Koizumi, K. *J. Antibiot.* **1976**, *29*, 1.
- Yoshida, M.; Kijima, M.; Akita, M.; Beppu, T. *J. Biol. Chem.* **1990**, *265*, 17174.
- (a) Richon, V. M.; Webb, Y.; Merger, R.; Sheppard, T.; Jursic, B.; Ngo, L.; Civoli, F.; Breslow, R.; Rifkind, R. A.; Marks, P. A. *Proc. Natl. Acad. Sci. U.S.A.* **1996**, *93*, 5705; (b) Marks, P. A. *Oncogene* **2007**, *26*, 1351.
- Miller, T. A.; Witter, D. J.; Belvedere, S. *J. Med. Chem.* **2003**, *46*, 5097.
- Cheson, B. D. *Br. J. Cancer* **2006**, *95*, S1.
- Finnin, M. S.; Donigian, J. R.; Cohen, A.; Richon, V. M.; Rifkind, R. A.; Marks, P. A.; Breslow, R.; Pavletich, N. P. *Nature* **1999**, *401*, 188.
- Somoza, J. R.; Skene, R. J.; Katz, B. A.; Mol, C.; Ho, J. D.; Jennings, A. J.; Luong, C.; Arvai, A.; Buggy, J. J.; Chi, E.; Tang, J.; Sang, B. C.; Verner, E.; Wynands, R.; Leahy, E. M.; Dougan, D. R.; Snell, G.; Navre, M.; Knuth, M. W.; Swanson, R. V.; McRee, D. E.; Tari, L. W. *Structure* **2004**, *12*, 1325.
- Vannini, A.; Volpari, C.; Filocamo, G.; Casavola, E. C.; Brunetti, M.; Renzoni, D.; Chakravarty, P.; Paolini, C.; De Francesco, R.; Gallinari, P.; Steinkuhler, C.; Di Marco, S. *Proc. Natl. Acad. Sci. U.S.A.* **2004**, *101*, 15064.
- Charrier, C.; Bertrand, P.; Gesson, J.-P.; Roche, J. *Bioorg. Med. Chem. Lett.* **2006**, *16*, 5339.
- Anandan, S. K.; Xiao, Z.-Y.; Patel, D. V.; Ward, J. S. US Patent 2005234033 A1 20051020.
- Delorme, D.; Woo, S. H.; Vaisburg, A.; Moradel, O.; Leit, S.; Raepfel, S.; Frechette, S.; Bouchan, G.; WO 03/024443 A3.
- Maguire, A. R.; Papot, S.; Ford, A.; Touhey, S.; O'Connor, S.; Clynes, M. *Synthesis* **2001**, *1*, 41.
- Ludwig, T.; Ermert, J.; Coenen, H. *Nucl. Med. Biol.* **2002**, *29*, 255.
- Lucet, D.; Heyse, P.; Gissot, A.; Le Gall, T.; Mioskowski, C. *Eur. J. Org. Chem.* **2000**, 3575.
- Liu, P.; Chen, Y.; Deng, J.; Tu, Y. *Synthesis* **2001**, *14*, 2078.
- Johnson, G. D.; Lindsey, W. B.; Jones, B. R. *J. Am. Chem. Soc.* **1956**, *78*, 461.
- Kahnberg, P.; Lucke, A. J.; Glenn, M. P.; Boyle, G. M.; Tyndall, J. A. D.; Parsons, P. G.; Fairlie, D. P. *J. Med. Chem.* **2006**, *49*, 7611.
- Protein surfaces of HDAC8 were obtained from corresponding pdb files, using internet Chime plugin from MDL. Theoretical calculations were realized at the AM1 level, using the closed shell (restricted) wave function from Chem3D facilities.